Materials Research Bulletin 64 (2015) 1–5

Contents lists available at ScienceDirect

Materials Research Bulletin

journal homepage: www.elsevier.com/locate/matresbu

Effect of Al_2O_3 insertion on the electrical properties of $SrTiO_3$ thin films: A comparison between Al_2O_3-doped $SrTiO_3$ and $SrTiO_3/Al_2O_3/SrTiO_3$ sandwich structure

Ji-Hoon Ahn [a], Ja-Yong Kim [b], Seong-Jun Jeong [a], Se-Hun Kwon [c,d,*]

[a] Samsung Advanced Institute of Technology, Samsung Electronics Corporation, Yongin-Si, Gyeonggi-Do 446-712, Republic of Korea
[b] Department of Materials Science and Engineering, Korea Advanced Institute of Science and Technology, 373-1, Guseong-dong, Yuseong-gu, Daejeon 305-701, Republic of Korea
[c] National Core Research Center for Hybrid Materials Solutions , Pusan National University, 30 Jangjeon-Dong Geumjeong-Gu, Busan 609-735, Republic of Korea
[d] School of Materials Science and Engineering, Pusan National University, 30 Jangjeon-Dong Geumjeong-Gu, Busan 609-735, Republic of Korea

ARTICLE INFO

Article history:
Received 20 May 2014
Received in revised form 4 November 2014
Accepted 3 December 2014
Available online 4 December 2014

Keywords:
A. Oxides
A. Thin flims
B. Vapor deposition
D. Dielectric properties

ABSTRACT

The effect of Al_2O_3 insertion on the electrical properties of $SrTiO_3$ films is systemically investigated in metal–insulator–metal (MIM) capacitor because $SrTiO_3$ films with a high dielectric constant generally suffer from high leakage current problem caused by grain boundaries and a narrow band gap. To find an effective Al_2O_3 insertion method, Al_2O_3 is inserted into $SrTiO_3$ thin films by two different ways. The first method is doping of Al_2O_3 in $SrTiO_3$ thin films and the second method is sandwiching a nanometer-thick Al_2O_3 layer between $SrTiO_3$ thin films. With respect to leakage blocking properties, the leakage current of Al_2O_3-doped $SrTiO_3$ films is effectively reduced when the $SrTiO_3$ film becomes amorphous by doping. In case of the $SrTiO_3/Al_2O_3/SrTiO_3$ structure, an Al_2O_3 layer with a thickness of more than 1.19 nm effectively acts as a leakage current blocking layer without $SrTiO_3$ amorphization. Moreover, the degradation of the dielectric properties of Al_2O_3-doped $SrTiO_3$ films is more severe, caused by structural degradation, than of $SrTiO_3/Al_2O_3/SrTiO_3$ structured films. Therefore, compared with Al_2O_3-doped $SrTiO_3$, a more than two times higher value (~45) of the dielectric constant can be obtained in the $SrTiO_3/Al_2O_3/SrTiO_3$ structured films with a similar leakage current density of 10^{-7} A/cm^2.

1. Introduction

Perovskite strontium titanate ($SrTiO_3$) thin films have been widely investigated in view of electronic applications such as ferroelectric film capacitors [1], tunable resonant circuits [2], non-volatile memories [3], optoelectronics [4] and, especially, high dielectric capacitors in dynamic random access memories [5–7] owing to their excellent dielectric properties. Excellent dielectric properties of $SrTiO_3$ films can be achieved if these films have a perovskite crystal structure. However, dielectric thin films with a high crystallinity generally have a lot of grain boundaries that act as conduction paths of leakage current. Therefore, $SrTiO_3$ thin films with a high dielectric constant suffer from high leakage current owing to internal grain boundaries and/or cracks [8] and, moreover, the narrow band gap of $SrTiO_3$ (about 3.3 eV) could also cause a high leakage current [9]. This leakage current problem challenges the practical application of $SrTiO_3$ films in microelectronic industry, especially with regard to MIM applications.

To improve the leakage current properties of high-*k* dielectrics, the introduction of various combinations of current barrier materials such as Al_2O_3, La_2O_3, and SiO_2 have been proposed in forms of stacked structures, intermixing structures, sandwich structures, and others [10–13]. Generally, the method of reducing the leakage current by the insertion of a current barrier material may accompany a problem of decreasing the capacitance, because leakage current barrier materials have relatively low dielectric constants. Therefore, it is necessary to investigate the variation of the electrical properties of a high-*k* material upon insertion of a current barrier material for various insertion methods. However, most of the researches have focused on the effect of an individual specific structure resulting in a lack of a comparative study between different structure combinations of high-*k* materials and current barrier material systems.

In this paper, the effect of alumina (Al_2O_3) insertion on the electrical properties of $SrTiO_3$ films was systemically investigated. To examine the variation of the electrical properties of Al_2O_3-added

---

* Corresponding author at: School of Materials Science and Engineering, Pusan National University, 30 Jangjeon-Dong Geumjeong-Gu, Busan 609-735, Republic of Korea. Tel.: +82 51 510 3775; fax: +82 51 518 3360.
E-mail address: sehun@pusan.ac.kr (S.-H. Kwon).

http://dx.doi.org/10.1016/j.materresbull.2014.12.012

$SrTiO_3$ films, Al_2O_3 was introduced into $SrTiO_3$ thin films by two different ways. The first method for reducing leakage current is doping of Al_2O_3 in $SrTiO_3$ thin films. Since Al_2O_3 films have excellent leakage current properties, it is anticipated that Al_2O_3-doped $SrTiO_3$ films will exhibit a reduced leakage current. The second method is the insertion of an Al_2O_3 layer with a thickness of the order of a few nanometer in between $SrTiO_3$ thin films (sandwiching the Al_2O_3 layer between $SrTiO_3$) as a leakage current blocking layer. It is expected that the thin Al_2O_3 layer with amorphous structure might act as a leakage current blocking layer in a crystalline $SrTiO_3$ thin film because Al_2O_3 has a high crystallization temperature (>900 °C) and a large band gap (about 8.7 eV) with a corresponding low leakage current [14].

2. Experimental details

Al_2O_3-added $SrTiO_3$ thin films were deposited on a $SrRuO_3$ seed layer using plasma-enhanced atomic layer deposition (PEALD) adopting a supercycle concept [15]. Before the Al_2O_3-added $SrTiO_3$ films were deposited, the $SrRuO_3$ seed layer was prepared by a 2.7 nm SrO layer on a 30-nm-thick bottom electrode of RuO_2 and post-annealing, as explained in an earlier report [16]. The deposition of SrO layers on top of $RuO_2/SiO_2/Si$ substrates by PEALD was followed by 10 min of annealing for a reaction of SrO and RuO_2 to form a $SrRuO_3$ layer under O_2 ambient at a temperature of 600 °C. Next, two types of Al_2O_3-added $SrTiO_3$ thin films were formed on the $SrRuO_3$ seed layer at a deposition temperature of 225 °C and a pressure of 3 Torr. The used precursors were $Sr(DPM)_2$ [$Sr(C_{11}H_{19}O_2)_2$] and TTIP [$Ti(O_i\text{-}C_3H_7)_4$] for $SrTiO_3$ deposition and TMA [$Al(CH_3)_3$] for Al_2O_3 addition. Oxygen plasma was used as an oxidant. $Sr(DPM)_2$ was dissolved in butyl acetate (0.2 M) and supplied to the reaction chamber by a liquid delivery system. TTIP vapor was carried in argon gas though a bubbler at 60 °C and TMA vapor was supplied without carrier gas to the reaction chamber while maintaining a vessel temperature of 30 °C. At a converged regime, the saturated growth rates of SrO, TiO_2, and Al_2O_3 films were 0.054, 0.036, and 0.11 nm/cycle, respectively. One supercycle for $SrTiO_3$ deposition was consisted of six TiO_2 cycles and seven SrO cycles in order to obtain a stoichiometric $SrTiO_3$ films (Sr:Ti = 1:1.03).

To investigate the impact of the structure of the leakage current barrier material on the electrical properties of Al_2O_3-added $SrTiO_3$ films, Al_2O_3 was inserted in two different ways, as shown Fig. 1 and Table 1. The first method is doping of Al_2O_3 in $SrTiO_3$ thin films (Al_2O_3-doped $SrTiO_3$) and the second method is sandwiching an Al_2O_3 layer between bottom and top $SrTiO_3$ thin films ($SrTiO_3/Al_2O_3/SrTiO_3$, sandwich). Applying the first method, a cycle for Al_2O_3 was periodically inserted during the $SrTiO_3$ deposition by varying the number of Al_2O_3 cycles (denoted by 'n') from 0 to 21. Concerning the second method, the process sequence was as follows. First, 10-nm-thick $SrTiO_3$ films were deposited on $SrRuO_3$ seed layers. Then, the Al_2O_3 layers were deposited on top of the $SrTiO_3$ films in a continuous manner by varying the number of deposition cycles ('n') from 5 to 20 (corresponding to a thickness range of about 0.6–2.4 nm). After that, 5-nm-thick $SrTiO_3$ films were deposited on the Al_2O_3 blocking layers; consequently, the sandwich structure of $SrTiO_3/Al_2O_3/SrTiO_3$ films was fabricated. For both methods, the number of supercycles (denoted by 'm') for the deposition of $SrTiO_3$ was fixed to 21 (one supercycle consisted of six TiO_2 and seven SrO cycles.) which resulted in 15-nm-thick stoichiometric $SrTiO_3$ films [15]. For crystallization, the as-deposited films underwent a rapid thermal annealing at 600 °C for 10 min under N_2 ambient. The film thickness was measured at a wavelength of 632.5 nm using an ellipsometer (Gaertner L116C) and X-ray diffraction (XRD, Rigaku) analysis using Cu Kα radiation (λ = 1.5405 Å) was carried out to investigate the crystal structures of the Al_2O_3-added $SrTiO_3$ thin films. To examine the electrical properties, 100-nm-thick Pt dots deposited by sputtering with a diameter of 160 μm were used as a top electrode and the dielectric constant was measured using a C–V analyzer (Keithley 590) at a frequency of 1 MHz.

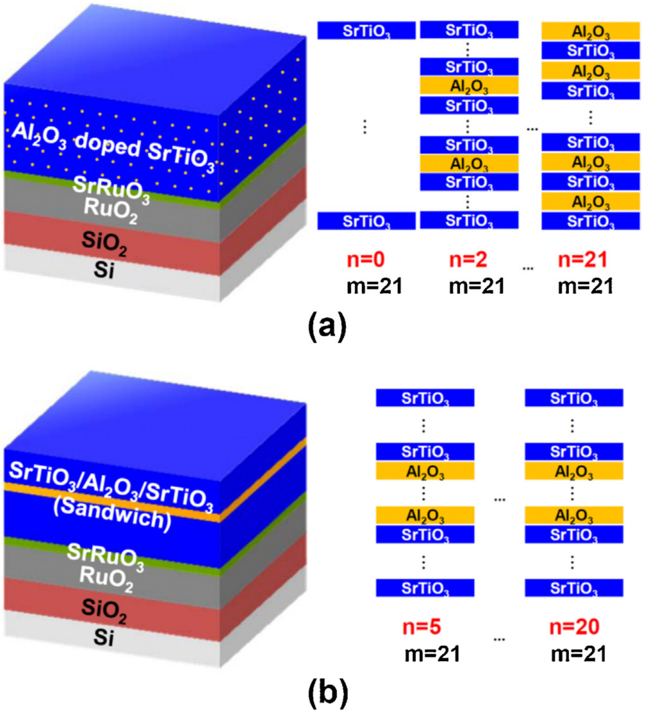

Fig. 1. Schematic diagrams of two different types of Al_2O_3-added $SrTiO_3$ films and the corresponding PEALD cycle sequences; (a) doping of Al_2O_3 in $SrTiO_3$ films (Al_2O_3-doped $SrTiO_3$), (b) sandwiching an Al_2O_3 layer between a bottom and a top $SrTiO_3$ film ($SrTiO_3/Al_2O_3/SrTiO_3$). The letter n and m denotes the number of Al_2O_3 cycles and $SrTiO_3$ supercycles, respectively.

3. Results and discussion

Fig. 2 demonstrates the variation of the total thickness of Al_2O_3-added $SrTiO_3$ films as a function of the number of Al_2O_3 cycles while keeping fixed the number of $SrTiO_3$ supercycles at 21. The total thickness linearly increased with the number of Al_2O_3 cycles and the deposition rates of Al_2O_3 in $SrTiO_3$ films obtained from the slope of the graph were very similar for direct doping and the sandwich structure (0.121 nm/cycle for doping and 0.119 nm/cycle for the sandwich structure). This means that the deposited

Table 1
A detailed summary of PEALD cycle sequences for Al_2O_3 added $SrTiO_3$ thin films.

Film structure	# of Al_2O_3 unitcycles	# of $SrTiO_3$ supercycles	PEALD cycle sequences*
$SrTiO_3$ thin films	n = 0	m = 21	STO*21
Al_2O_3-doped $SrTiO_3$ thin films	n = 2	m = 21	(STO*7)-(AO*1)-(STO*7)-(AO*1)-(STO*7)
	n = 4	m = 21	[{(STO*4)-(AO*1)}*4]-(STO*5)
	n = 7	m = 21	[{(STO*3)-(AO*1)}*7]
	n = 10	m = 21	[{(STO*2)-(AO*1)}*10]-(STO*1)
	n = 21	m = 21	[{(STO*1)-(AO*1)}*21]
$SrTiO_3/Al_2O_3/SrTiO_3$ sandwiched thin films	n = 5	m = 21	(STO*14)-(AO*5)-(STO*7)
	n = 10	m = 21	(STO*14)-(AO*10)-(STO*7)
	n = 15	m = 21	(STO*14)-(AO*15)-(STO*7)
	n = 20	m = 21	(STO*14)-(AO*20)-(STO*7)

*STO: one supercycle for $SrTiO_3$ deposition; AO: one cycle for Al_2O_3 deposition.